SCIENCE CHINA
Information Sciences

• RESEARCH PAPER •
Special Focus on Cyber-Physical Systems

January 2022, Vol. 65 110204:1–110204:16
https://doi.org/10.1007/s11432-020-3344-8

Wireless/wired integrated transmission for industrial cyber-physical systems: risk-sensitive co-design of 5G and TSN protocols

Yajing ZHANG[1,2,3†], Qimin XU[1,2,3†], Xinping GUAN[1,2,3*],
Cailian CHEN[1,2,3] & Mingyan LI[1,2,3,4]

[1] *Department of Automation, Shanghai Jiao Tong University, Shanghai* 200240*, China;*
[2] *Key Laboratory of System Control and Information Processing, Ministry of Education of China, Shanghai* 200240*, China;*
[3] *Shanghai Engineering Research Center of Intelligent Control and Management, Shanghai* 200240*, China;*
[4] *College of Computer Science, Chongqing University, Chongqing* 400044*, China*

Received 15 September 2020/Revised 19 July 2021/Accepted 27 September 2021/Published online 27 December 2021

Abstract The growing popularity of intelligent manufacturing is driven by deterministic transmission demands of applications in industrial cyber-physical systems (ICPS). However, the ossified shortages of industrial wireless communication such as diverse quality of service (QoS) and complex signaling processes incur a severe long tail of transmission delay distribution. As a solution, the 5th generation (5G) wireless communication technology provides ultra-reliable and low-latency communication (URLLC) for industry scenarios. Moreover, the newly proposed time-sensitive networking (TSN) standards guarantee the transmission determinacy by gate mechanism. In this paper, we propose a heterogeneous time-sensitive network (HTSN) co-designed by 5G and TSN. We first develop a predictive multi-priority wireless scheduling mechanism based on semi-persistent scheduling (SPS) to reduce signaling delay by reserving resources in advance. Then we propose an adaptive data injection mechanism for TSN based on per-stream filtering and policing (PSFP), which dynamically adjusts the priority of data for queue injection in TSN. To further reduce the long tail of delay, we employ a risk-sensitive learning method to improve the worst-case delay. Simulations on a hot rolling production scenario demonstrate that the proposed mechanisms under HTSN achieve great performance in terms of integrated delay and resource utilization.

Keywords industrial cyber-physical systems (ICPS), 5G-TSN co-design, wireless/wired integrated network, risk-sensitive reinforcement learning, deterministic communication

Citation Zhang Y J, Xu Q M, Guan X P, et al. Wireless/wired integrated transmission for industrial cyber-physical systems: risk-sensitive co-design of 5G and TSN protocols. Sci China Inf Sci, 2022, 65(1): 110204, https://doi.org/10.1007/s11432-020-3344-8

1 Introduction

With the promotion of the fourth industrial revolution (also known as industry 4.0), manufacturing is converted from traditional industrial automation to intelligent manufacturing, where the latter integrates a huge amount of devices that are embedded and networked together in industrial cyber-physical systems (ICPS) [1]. To improve the manufacturing performance of ICPS, such as real-time monitoring and control, deterministic communication is imperative from the industry field to the data center in order to provide online control for the control system. In particular, the automatic control system has a stringent timeliness request, where violating a deadline may severely damage the control quality and even result in serious economic and safety problems. However, the diversity of CPS applications makes it intractable to meet their quality-of-service (QoS) demands timely [2].

As a new generation of wireless communication, the 5th generation (5G) wireless communication technology is expected to expand industrial informatics and automation into much broader contexts [3].

* Corresponding author (email: xpguan@sjtu.edu.cn)
† Zhang Y J and Xu Q M have the same contribution to this work.

Among several typical usage scenarios of 5G, ultra-reliable and low latency communication (URLLC) has the characteristics of high reliability up to 99.9999% and low delay down to millisecond [4], which is appropriate for intelligent manufacturing, smart grid, and other automatic control scenarios that require extremely high reliability as well as ultra-low latency. Besides, massive machine type communication (mMTC) is another target scenario for 5G, which is designed for massive data monitoring and collection in ICPS. Unfortunately, there are three main challenges to apply 5G technology to the ICPS. (1) Due to the complex signaling process of the dynamic access mechanism, the conventional cellular network fails to guarantee the strict timelines of industrial automation. (2) The ICPS have many characteristics such as the complex communication environment, limited radio resources, and severe interference, which lead to the long tail effect of the delay distribution. (3) Data's QoS requirements are diverse and the dynamic burst data always carry safety information, which make it intractable to deliver data on demand.

Contrary to the 5G technology, time-sensitive networking (TSN) standards ensure the determinacy and reliability of its innovative mechanisms such as gate control list (GCL) and time-aware shaper (TAS), which are suitable for URLLC scenarios. Moreover, TSN gateways can deliver data in a guaranteed time window with bounded latency, small jitter, and extremely low data loss [5]. However, TSN is designed for standard ethernet, which has the inherent shortcomings of wired transmission, such as the limited coverage, the higher cost of maintenance, and the complexity of installation.

Example 1. Taking the hot rolling process as an example, it roughly includes five steps: heating, milling, colling, coiling and delivering. Sensors are randomly distributed among the whole rolling process, fixed large equipment (such as the furnace, the charge machine, the down coiler) and flexible mobile devices (such as automated guided vehicles, AGV) work together, and staffs operate in order. If the periodic vibration data are not timely delivered via 5G due to the severe industrial electromagnetic interference, the thickness of the slab will not be uniform since the mill cannot control it without the feedback data. Moreover, it is unnecessary for the furnace and other fixed equipment to communicate with others via 5G as sensors need to be charged frequently. 5G network is more suitable for mobile devices. In addition, as the main communication mode in the current industry, the industrial ethernet is compatible with TSN, while it may incur a high upgrade cost to completely use 5G.

Therefore, it is inevitable to propose a more flexible and deterministic transmission architecture to meet the strict requirements of intelligent manufacturing via 5G and TSN. To address this problem, we propose a heterogeneous time-sensitive network (HTSN), a heterogeneous architecture integrating 5G and TSN. The contributions of this paper are summarized as follows.

(1) HTSN: a heterogeneous 5G-TSN integrated architecture. To provide flexible and deterministic transmission, we propose a heterogeneous architecture HTSN, which flexibly guides data to access the TSN gateway via the 5G network and forwards deterministically within the TSN network. This architecture has both advantages of 5G and TSN and can deliver data timely after the adjustment in 5G and TSN, respectively.

(2) Predictive multi-priority wireless scheduling mechanism. Considering the limited resources of ICPS, we design a preemption-based predictive multi-priority wireless scheduling mechanism on the basis of semi-persistent scheduling (SPS). In particular, limited resources are reserved for sensors beforehand according to their triggering correlations. Thus, the handshaking delay is reduced and the resource utilization is improved.

(3) Adaptive data injection mechanism from 5G to TSN. To deal with the interference of the industrial wireless environment, we propose an adaptive data injection mechanism based on the per-stream filtering and policing (PSFP) mechanism of TSN to offset the jitter caused by the 5G network. The relationship between the priority of queues and the transmission delay through TSN is given to adjust the priority of data when they are injected into the TSN network.

(4) Risk-sensitive learning strategy for wireless scheduling and data injection. In consideration of the long tail of the transmission delay, a risk-sensitive utility function is proposed, which consists of the expectation, variance, and third-order central moment of the total delay. Leveraging reinforcement learning to adjust the number of reserved resource blocks (RB) and the TSN injection queue, the delay distribution is more centralized with a shorter tail. Thus, the diverse QoS requirements of data are satisfied and the centralized delay distribution brings a more reliable transmission.

The remainder of this paper is organized as follows. In Section 2, we introduce the related work of the heterogeneous network and real-time scheduling, and then we give the overview of our HTSN in Section 3. In Section 4, we introduce the system model and formulate the optimization objective. Then we present the risk-sensitive learning strategy and simulation results in Sections 5 and 6, respectively. Finally, this paper is concluded in Section 7.

2 Related work

The smart factory has received increasing attention for its strict communication demand of lower latency and higher reliability. The accompanying problem is how to improve the transmission determinacy of end-to-end (E2E) delay from the industry field to the data center under our HTSN, which brings two main issues to focus on: the deterministic transmission via a heterogeneous network and the low access delay of the wireless network. Therefore, the related work is concluded in two aspects as mentioned above.

2.1 Heterogeneous network architecture

2.1.1 *Wireless/wired hybrid network*

In recent years, the combination of wireless and wired networks has attracted significant attention [6–9]. The authors in [6, 7] concentrated on using software-defined networking (SDN) to provide centralized control of the wireless/wired network. Ref. [6] proposed a network architecture where wireless and wired transmissions are used in parallel to make up for the shortcomings of the other one. Ref. [7] proposed a multi-path transmission mechanism under the architecture from wired to wireless to promote the video's transmission performance. Except for SDN, Ref. [8] proposed a protocol to support multimedia data in hybrid wireless/wired networks, which efficiently utilizes the wireless link with coexisting TCP flows and can provide satisfactory QoS for delay-sensitive multimedia applications. As for the industry, Ref. [9] pointed out that since current wireless networks are not suitable to fulfill the applications' requirements, hybrid wired-wireless networks have to be developed in order to support the implementation of ICPS. However, these studies only focus on the hybrid transmission based on the traditional TCP/IP network while the coming 5G and TSN are more suitable for industrial communication.

2.1.2 *5G-TSN integrated network*

The TSN industry white paper recently points out that the URLLC scenario of 5G is the key to realizing the industrial internet. How to deeply combine 5G and TSN is the research hotspot. For this issue, Ericsson proposes a 5G-TSN integration conception in [5], where the SDN controller manages the whole network, and TSN protocols are applied in 5G users to guarantee strict E2E delay demands. Furthermore, Ericsson thinks that the integration of URLLC in the manufacturing process has great potential to accelerate the transformation of the manufacturing industry [10]. Nevertheless, these combinations of 5G and TSN are only preliminary ideas that still have a long way to be implemented.

2.2 Real-time scheduling of wireless communications

2.2.1 *Risk-sensitive transmission*

As stated in Section 1, the risk is a notion in financial mathematics [11], which we use to measure the risk of transmission delay. For wireless communication, the risk is equivalent to the loss of valuable information due to the instability and randomness of wireless transmission. For example, the quality of the stochastic channel may cause a variation of latency, which will incur emergency information lost when the variation is higher [12]. What is more, some fine-grained characteristics of delay in queueing networks, such as the delay distribution and probability boundary (the tail of delay), are critical while most studies only care about the average delay rather than the worst delay [13]. In existing studies, Refs. [14, 15] studied URLLC and low-latency communication to evaluate the performance under the influence of data dispersion and network density. They all focus on maximizing the average delay of network throughput or minimizing the average latency without providing any guarantee of the higher moment such as variance, skewness, kurtosis. Refs. [16, 17] took the mean and variance of delay account to capture the tail of delay and optimize the bandwidth and transmission power without considering frequency diversity. To maximize the throughput of eMBB data, Ref. [18] took burst URLLC data into account and assumed it is a Rayleigh distribution, while the burst data are actually dynamic sporadic.

2.2.2 *Semi-persistent scheduling*

Due to the complex "scheduling request-scheduling grant (SR-SG)" signaling mechanism, the conventional dynamic access scheme of the cellular network cannot satisfy the strict delay requirements [19]. To this end, a fast uplink access scheme based on SPS is proposed in LTE Release 13 [20]. Thus the uplink resources are assigned in advance to reduce the "SR-SG" overhead, which is suitable for machine-type communications (MTC) in industrial automation [21]. However, SPS is designed for VoIP originally, the transmission of which is fixed and known, while the QoS of MTC devices varies, and the scheduling request is time-varying and even dynamic sporadic [22]. For this, Ref. [23] proposed an adaptive SPS scheme to adjust the resources in the next transmission by buffer report. Moreover, to make further use of unused resources, other devices can be assigned partial resources in a semi-persistent way based on a device-to-device (D2D) manner, which can lead to extra latency [24].

2.2.3 *Multi-priority wireless transmission*

In industrial wireless networks (IWNs), the priority of data can be established according to the requirements of applications [25]. Thus the essential requirement of IWNs is to support the transmission of mixed-priority data that have different demands of latency and reliability [26, 27]. For example, as mentioned in [28], there are four different types of information in the industry: the safety/emergency information which requires the highest reliability and the lowest latency, the regulate/monitor control information which possesses the lenient requirements, the open-loop control information which allows minute-level delay, and the monitoring information which has no requirements. To deal with this problem, Ref. [29] proposed a time division multiple access (TDMA)-based multichannel superframe strategy to keep the superiority of each priority with full radio channel reuse while the strategy is implemented for cluster-based IWN without considering burst data. Similarly, a multi-priority scheme named p-persistent is proposed in [30] based on carrier sense multiple access (CSMA), which guarantees the transmission of high priority at the expense of longer delay of low priority data and still does not take burst data into account.

In conclusion, although optimizing wireless transmission has been well studied, it is still a big challenge to apply it to industrial automation. Moreover, the integration of 5G and TSN is a promising trend for intelligent manufacturing.

3 Overview of HTSN

As illustrated in Figure 1, the architecture of HTSN consists of two coupling stages: the 5G network and the TSN network. The 5G network is composed by a set of $\mathcal{S} = (s_1, s_2, \ldots, s_{|S|})$ sensors, communication nodes and controllers, etc. Different sensors collect different types of data. The TSN consists of a set of TSN gateways which also work as 5G base stations (BSs). The BSs are in charge of the assignment of the RBs $\mathcal{R} = (r_1, r_2, \ldots, r_{|R|})$, where one RB denotes a series of time-frequency domain radio resource blocks and is sufficient to transmit most of the data collected by sensors. RB's corresponding time period, denoted by subslot, is the minimum non-divisible time unit in 5G. The frequency band of one RB represents a channel, which is flat fading and homogeneous. In more detail, the time-frequency resources of one RB mean that we can use the frequency band for a period of time (referred to as the channel and the subslot mentioned before). We divide the RB pool into three parts: predictive reserved RBs, RBs for signal transmission, and RBs for dynamic access. The industrial field data from different sensors (temperature sensors, vibration sensors) are transmitted through shared RBs to TSN gateways, and then are sent to the remote data center via wired TSN.

Due to the diverse QoS requirements of field data, it is divided into three types. (1) Non-scheduled (NS) data, which is sporadically triggered by the emergency event and has the highest priority. (2) Time-critical (TC) data, which is the typical type of data in industrial automation and the amount of which is much larger than that of NS data. (3) Best-effort (BE) data, which has the lowest priority and follows the best-effort forwarding rules. In industry, such as a hot rolling production process, data are transmitted periodically, so we only consider the transmission in one time period, denoted by transmission time interval (TTI), which consists of 5G and TSN parts. The whole cycle of industrial automation can be regarded as the accumulation of TTIs. In each TTI of 5G, we first select the nodes that are most likely to trigger, and then we assign the TC data collected by these nodes on predictive reserved RBs

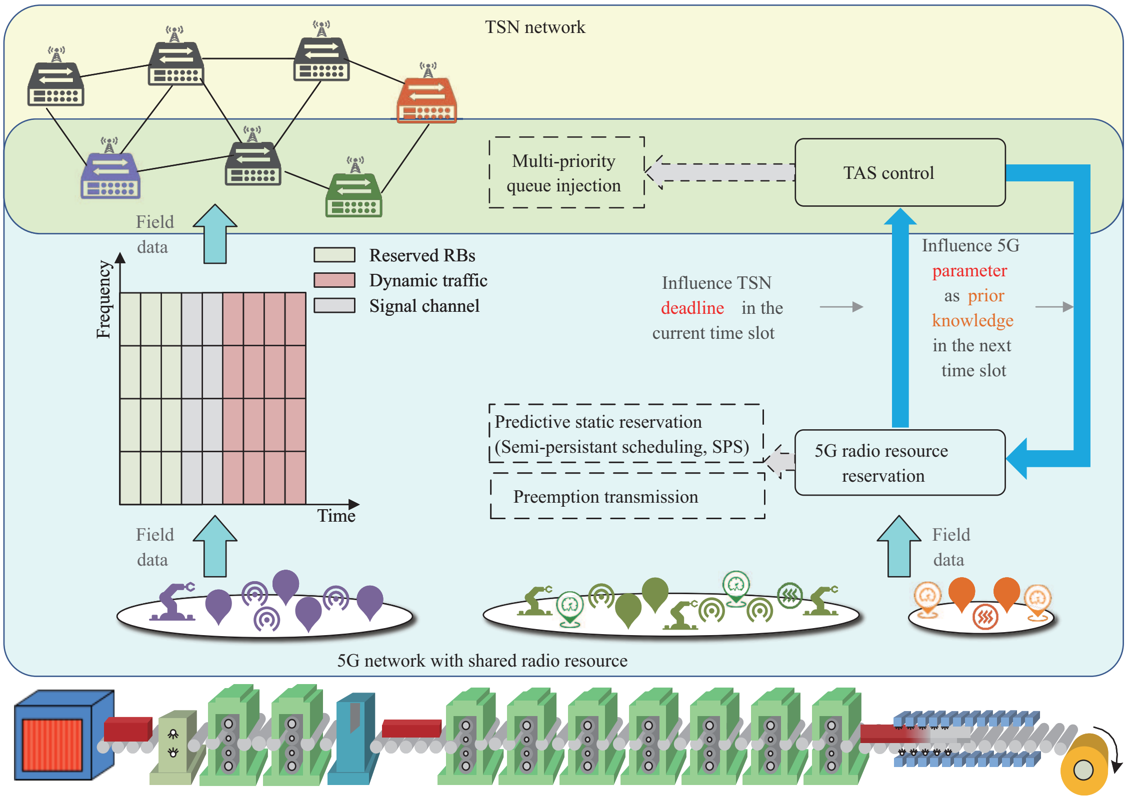

Figure 1 (Color online) The architecture of HTSN.

based on the SPS technique to omit handshaking (signaling) delay. The residual TC data and BE data are served on dynamic RBs by the conventional dynamic access procedure orderly, which consists of handshaking in signaling procedure of transmission process. The difference between predictive reserved RBs and dynamic RBs is that the reserved RBs are assigned to sensors in advance without explicit SR-SG signaling procedure. Considering the highest priority and the sporadically triggered feature of NS data, we set a fixed reserved RB at each subslot for possible NS data. To improve the utilization of RBs, the fixed reserved RBs can be used by TC data and BE data with no NS data arriving. And NS data can preempt any data as soon as they arrive. Note that the priority of NS data is the same as that of TC data after it is embedded in the 5G network.

Based on the PSFP mechanism in the IEEE 802.1Qci protocol, TSN gateways assign different gate IDs to data according to their transmission delay in 5G and the total delay demand. Data arrived at the gateway are injected into the gateway's sending queue that matches its gate ID assigned before. Thus, data from the 5G network are scheduled differentially in the TSN to meet their diverse QoS requirements and achieve time-sensitive transmission under HTSN.

Specifically, the delay of the TC data (including arrived NS data) across 5G network and TSN network in TTI t, denoted by $T_{5\mathrm{G}}(t)$ and $T_{\mathrm{TSN}}(t)$, respectively, is coupled. Note that the E2E delay of TC data from the industrial field to the remote data center can be calculated as $T_{\mathrm{E2E}}(t) = T_{5\mathrm{G}}(t) + T_{\mathrm{TSN}}(t)$. In each TTI, the total amount of RBs is fixed, so that the larger amount of predictivel reserved RBs $|\mathcal{R}_{\mathrm{r}}(t)|$ in TTI t, the smaller the number of RBs for dynamic access. Note that $|\mathcal{R}_{\mathrm{r}}(t)|$ is much smaller than the number of sensors in field (i.e., $|\mathcal{R}_{\mathrm{r}}(t)| \ll |\mathcal{S}|$). If $T_{5\mathrm{G}}(t)$ of TC data is larger than excepted, it should be injected into a high priority queue $Q(t)$ of TSN gateways to offset the time deviation caused by 5G stage. Otherwise, data that have low 5G delay can be injected into low priority TSN queue to reserve resources for other data. Here, we aim to minimize the E2E delay of TC data, so it is necessary to consider both the $T_{5\mathrm{G}}(t)$ and the $T_{\mathrm{TSN}}(t)$ simultaneously.

Example 2. We take the rolling production process as an illustration. As shown in Figure 1, the 5G BS is installed in the TSN gateway as a local control center with learning ability. At the beginning of each TTI, the BS decides the number of reserved RBs according to the history data (the accumulated $T_{\mathrm{E2E}}(t)$). Then sensors correlated with the sensors that activated before are assigned to predictive reserved RBs and

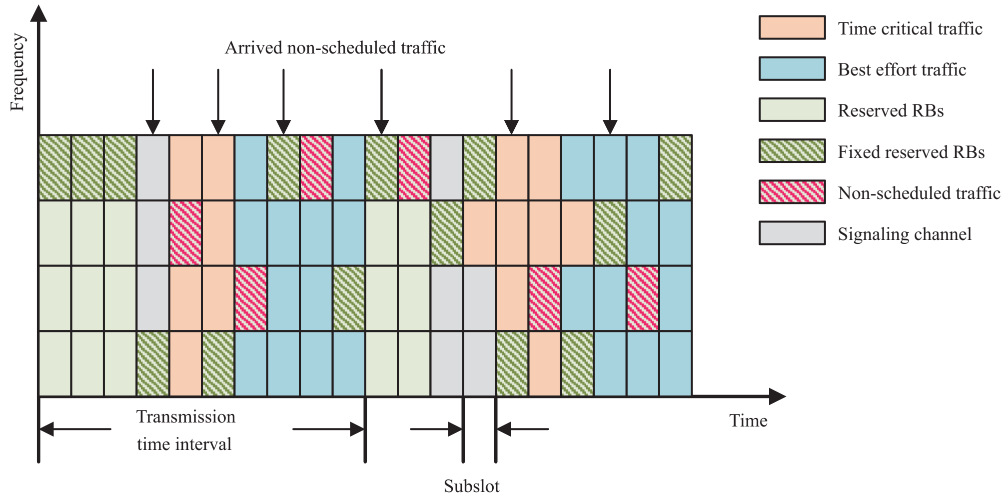

Figure 2 (Color online) The embedment of multi-priority data in 5G network.

execute the signaling procedure in advance. After that, the residual sensors dynamically access BSs with handshaking delay, and thus 5G delay $T_{5\mathrm{G}}(t)$ can be calculated according to the transmission state in 5G. Based on $T_{5\mathrm{G}}(t)$ and the QoS requirement of data, the BS decides the gate ID of the TSN gateway's queue that data will inject into.

4 System model

4.1 Multi-priority transmission model based on SPS

As discussed in Section 3, there are three issues of the 5G network: (1) predictive assign sensors that are the most correlated, (2) embed sensors obeying their diverse QoS requirements, and (3) preemption of TC data when NS data arrive. To this end, a preemption-based predictive multi-priority scheduling mechanism is proposed in this subsection. The predictive sensor selection policy will be expounded in Subsection 5.1 later.

As mentioned before, in intelligent manufacturing, a massive amount of data with diverse QoS requirements are generating all the time, which should be served on their time demand. However, the complex uplink "SR-SG" signaling process brings extra delay for handshaking. As a solution, reserving RBs to correlated sensors in advance without a signaling procedure is a suitable way to reduce transmission time. Even so, the urgent and critical data may still have an additional queuing delay due to the shortage of time-frequency radio resources in the factory. To this end, a preemption mechanism is proposed in this paper, which permits NS data to preempt TC data and BE data in order to realize no-wait transmission as soon as they arrive.

According to the QoS demands of data, we split radio resources into four parts in time order: predictive reserved RBs $\mathcal{R}_\mathrm{r}(\mathcal{R}_\mathrm{r} \subset \mathcal{R}$, referred to as reservation area), RBs for signaling transmission, RBs to transmit TC data dynamically, RBs to transmit BE data dynamically, as shown in Figure 2. Taking NS data that carry safety information into account, we set one fixed reserved RB dedicated to NS data at each subslot. There comes a problem: what will happen if the NS data arrive while the fixed reserved RB has already been allocated to the other data? That should be discussed according to whether the assigned sensor is triggered in Table 1, where $r_{\mathrm{brt},i}(t)$ denotes fixed reserved RB at the i-th subslot of TTI t, $s_i(t)$ denotes the sensor assigned to $r_{\mathrm{brt},i}(t)$, $\varphi(t) = \sum_{i=1}^{|\mathcal{R}_\mathrm{r}(t)|/|C|} \varphi_i$ denotes the number of fixed reserved RBs in reservation area, to which the sensors assigned are triggered, $\zeta(t) = \sum_{i=1}^{|\mathcal{R}_\mathrm{r}(t)|/|C|} \zeta_i$ denotes the number of arrived NS data in reservation area, and $\gamma(t) = \sum_{i=1}^{|\mathcal{R}_\mathrm{r}(t)|/|C|} \gamma_i$ denotes the number of fixed reserved RBs that is preempted by NS data while sensors assigned to them are triggered as well. Note that $C = \{c_1, c_2, c_3, \ldots\}$ is the set of channels and the number of channels is $|C|$.

Therefore, the number of RBs whose sensors are neither triggered nor preempted in the reservation area can be

$$|\mathcal{R}_\mathrm{r}(t)| - (|\mathcal{S}_\mathrm{e}(t)| + \zeta(t) - \gamma(t)), \tag{1}$$

Table 1 The condition of preemption and triggering on fixed reserved RBs

$\gamma_i = \zeta_i \varphi_i$	1	0
ζ_i	$r_{\text{brt},i}(t)$ is preempted	$r_{\text{brt},i}(t)$ is not preempted
φ_i	$s_i(t)$ is triggered	$s_i(t)$ is not triggered

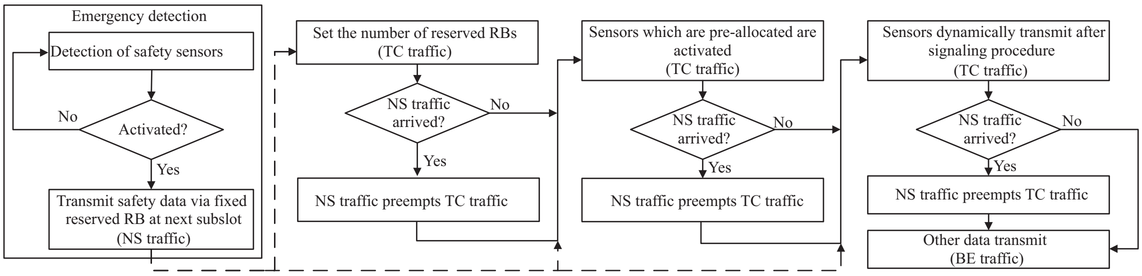

Figure 3 The process of multi-priority data transmission with preemption considered.

where $|\mathcal{S}_{\rm e}(t)|$ is the number of the TC data that embedded in the reservation area. Thus the total number of high priority sensors at TTI t, including TC data and embedded NS data, is given by

$$\begin{aligned}|\mathcal{S}_{\rm h}(t)| &= |\mathcal{R}_{\rm r}(t)| - (|\mathcal{R}_{\rm r}(t)| - (|\mathcal{S}_{\rm e}(t)| + \zeta(t) - \gamma(t))) + |\mathcal{S}_{\rm c}(t)| + |\mathcal{S}_{\rm b}(t)| - \zeta(t)\\ &= |\mathcal{S}_{\rm e}(t)| + |\mathcal{S}_{\rm c}(t)| + |\mathcal{S}_{\rm b}(t)| + \varphi(t) - \gamma(t),\end{aligned} \tag{2}$$

where $|\mathcal{S}_{\rm h}(t)|$ is the total number of high priority sensors (TC data and embedded NS data) scheduled at TTI t, $|\mathcal{S}_{\rm c}(t)|$ and $|\mathcal{S}_{\rm b}(t)|$ are the number of sensors generating TC data for dynamic access and the number of sensors generating NS data, respectively.

Ignoring the preemption of NS data, sensors pre-allocated to reserved RBs are scheduled firstly, followed by dynamic access sensors with extra signaling delay, and the BE data are scheduled in the end if there are any resources left. The whole transmission process is shown in Figure 3. It is worth mentioning that we here only focus on the delay of TC data, which is the time difference between the last served TC data and the beginning of the current TTI. The 5G delay can be calculated as follows:

$$T_{\rm 5G}(t) = \left\lceil \frac{|\mathcal{R}_{\rm r}(t)| + (|S_{\rm c}(t)| + |S_{\rm b}(t)| - (\zeta(t) - \gamma(t)))(1+\delta)}{|C|} \right\rceil \times T_{\rm RB}, \tag{3}$$

where $T_{\rm RB}$ is the time duration corresponding to one RB, δ is the proportion of signaling in the overall transmission, and $\lceil * \rceil$ represents the smallest integer which $*$ is less than or equal to. It can be seen from Figure 2 that if the last TC sensor is left in the last column alone, the 5G delay still needs to be extended for one $T_{\rm RB}$.

4.2 Data injection model of TSN gateways

As mentioned in Section 3, there are several sending queues in each port of TSN gateways, which have different transmission priorities. The coordination of TAS and GCL can make sure the data forwarded in TSN are deterministically delivered within their time demand while keeping the priority.

The PSFP mechanism proposed by IEEE 802.1Qci points out that each piece of data arrived owns a priority number, named internal priority values (IPV), which is related to its QoS demands and serves as a reference to transmit data heterogeneously in TSN. In detail, every piece of data will be assigned a gate ID to match its IPV number, where each gate ID represents a TSN sending queue, so the data with different IPV will be injected into different TSN queues. It can be seen that the key to deciding which queue to inject is the value of IPV, so we propose a data injection mechanism of TSN gateways based on IPV to offset the time deviation, such as jitters, caused by the 5G network. Thus, the TSN delay is adjusted according to the 5G network delay. Note that the data with a lower IPV number has higher priority.

Outlined in Figure 4, the data from the 5G network will be firstly gathered into a frame pool, where data generated within a TTI are classified into different priorities (referred to as IPV numbers) according to their 5G delay, and then injected into different TSN queues dynamically.

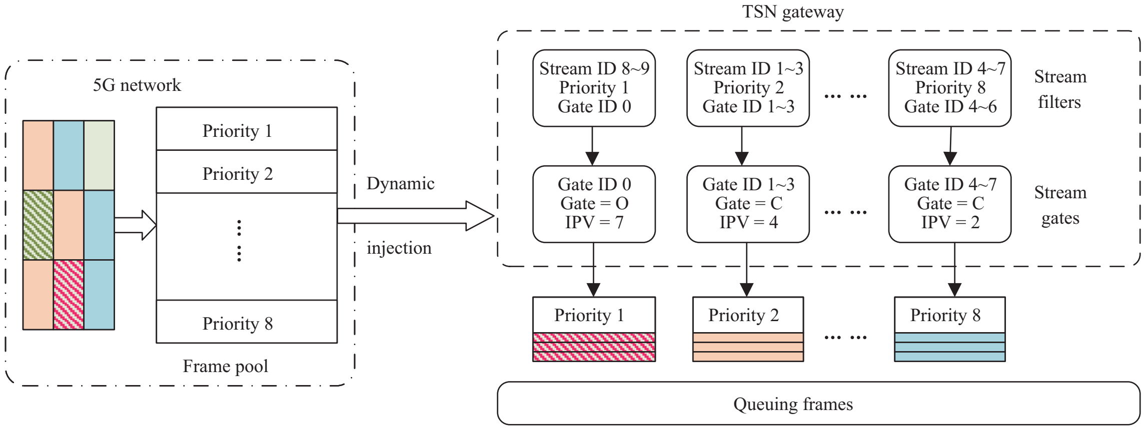

Figure 4 (Color online) Injection policy of TSN queue based on PSFP.

First, we divide the forwarding delay of TC data via TSN into x parts:

$$\Delta = \frac{T_{\rm TSN}^{\max} - T_{\rm TSN}^{\min}}{x}, \quad x = 1, 2, \ldots, \tag{4}$$

where $T_{\rm TSN}^{\max}$ and $T_{\rm TSN}^{\min}$ denote the maximum and the minimum forwarding delay through TSN, respectively, and x is the number of queues of a TSN port, which is usually eight.

Thus we can get the forwarding deadline of each queue as follows:

$$\Lambda\left(Q(t)\right) = T_{\rm TSN}^{\min} + Q(t) \times \Delta, \quad Q(t) = 1, 2, \ldots, x, \tag{5}$$

where $Q(t)$ is the gate ID of TSN queues, which is related to the IPV number of the arriving data from 5G at TTI t. In other words, the transmission threshold of the queue $Q(t)$ can be calculated by $(T_{\rm TSN}^{\min} + (Q(t) - 1) \times \Delta, T_{\rm TSN}^{\min} + Q(t) \times \Delta]$, which represents the scheduling capacity of TSN queue $Q(t)$ and means that it can afford the TC data of which the deadline within $Q(t)$'s capacity. Therefore, we get the forwarding deadline function of $Q(t)$, which can be used to calculate the delay of TSN and get the number of $Q(t)$ in reverse.

The TSN deadline with different queues is given by

$$T_{\rm TSN}(t) = H \left\lceil \frac{|\mathcal{S}_{\rm h}(t)| \times D \times \Lambda\left(Q(t)\right)}{\theta_{\rm low} T_{\rm cyc}} \right\rceil T_{\rm cyc}, \tag{6}$$

where $|\mathcal{S}_{\rm h}(t)|$ has been given in Subsection 4.1, H is the number of hops within TSN with fixed starting node and terminal, D is the fixed amount of data that one RB transmits, $T_{\rm cyc}$ is the forwarding cycle of TSN gateways, and $\theta_{\rm low}$ is the lowest data rate of TSN.

Based on the TSN deadline we get above, the value of $Q(t)$ is obtained by $\Lambda\left(Q(t)\right)$ as follows:

$$Q(t) = \arg \min_{1 \leqslant Q(t) \leqslant x} \left(T_{\rm TSN}(t) - \left(T_{\rm ddl}(t) - T_{\rm 5G}(t)\right)\right), \tag{7}$$

where $T_{\rm ddl}(t)$ is the delay demand of TC data arrived at TTI t, and $T_{\rm 5G}(t)$ is the transmission delay through previous 5G network.

Thus the entire transmission delay under HTSN at TTI t is given by

$$T_{\rm E2E}\left(T_{\rm 5G}(t), T_{\rm TSN}(t)\right) = T_{\rm 5G}(t) + T_{\rm TSN}\left(Q(t), \mathcal{F}\left(T_{\rm 5G}(t)\right)\right). \tag{8}$$

Example 3. Obviously, the delay of 5G network $T_{\rm 5G}(t-1)$ and the delay of TSN $T_{\rm TSN}(t-1)$ are coupling and interact with each other as shown in Figure 5. In particular, we first take the cumulative transmission delay $\sum_{m=1}^{t-2} T_{\rm E2E}(m)$ as prior information to obtain the number of reserved RBs $\mathcal{R}_{\rm r}(t-1)$ at TTI $t-1$. Then according to the 5G delay calculated by $\mathcal{R}_{\rm r}(t-1)$ and the coupling relationship between 5G delay and TSN delay, we can get the IPV number of TC data based on the data injection mechanism above. Finally, on the basis of the newly got $T_{\rm 5G}(t-1)$ and $T_{\rm TSN}(t-1)$, we can get the entire transmission delay $T_{\rm E2E}(t-1)$ under HTSN at TTI $t-1$, whereby it can be added into the cumulative transmission delay to get $\sum_{m=1}^{t-1} T_{\rm E2E}(m)$ and become the prior information of TC data in TTI t.

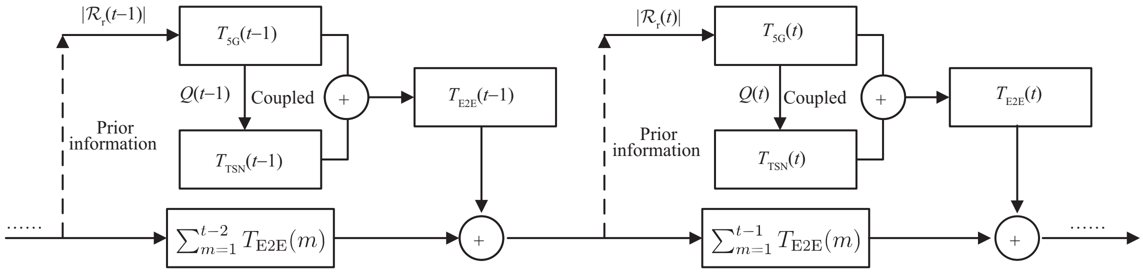

Figure 5 The operation process of TC data between TTIs under HTSN.

4.3 Risk-sensitive utility formulation

Considering the unreliability caused by the long tail of the 5G network delay, the higher-order quantity of wireless delay should be involved in the optimal problem as mentioned in Section 1. In this regard, we apply entropic risk measure $\frac{1}{\rho}\ln\left(\mathbb{E}\left[\exp\left(\rho T\right)\right]\right)$ and formulate a risk-sensitive minimization utility function of the entire transmission delay under HTSN as follows [13]:

$$\begin{aligned}\boldsymbol{\mathcal{P}1:}\ &\min_{\{|\mathcal{R}_{\rm r}(t)|,Q(t)\}}\frac{1}{\rho}\ln\left(\mathbb{E}\left[\exp\left(\rho\sum_{m=1}^{t-1}T_{\rm E2E}(m)\right)\right]\right)\\ &\text{s.t.}\ \ |\mathcal{R}_{\rm r}(t)|\leqslant\left|\Pi^{\rm sel}\right|,\\ &\qquad 1\leqslant Q(t)\leqslant 8,\end{aligned}\tag{9}$$

where $\mathbb{E}[*]$ is the expectation operator, $\left|\Pi^{\rm sel}\right|$ represents the number of predictive selected candidate sensors which is described in detail in Subsection 5.1.

The entropic risk measure $\frac{1}{\rho}\ln\left(\mathbb{E}\left[\exp\left(\rho\mathcal{T}\right)\right]\right)$ can be expanded out as $\frac{1}{\rho}\ln(\mathbb{E}[\exp(\rho\mathcal{T})]) = \mathbb{E}[\mathcal{T}] + \frac{\rho}{2!}\operatorname{Var}(\mathcal{T}) + \frac{\rho^2}{3!}\mathbb{E}\left[(\mathcal{T}-\mathbb{E}[\mathcal{T}])^3\right]+\cdots$, where $\mathcal{T}$ denotes the cumulative time $\sum_{m=1}^{t-1}T_{\rm E2E}(m)$. It is obvious that the optimal objective takes into account the variance $\operatorname{Var}(\mathcal{T})$ and the third central moment $\mathbb{E}\left[(\mathcal{T}-\mathbb{E}[\mathcal{T}])^3\right]$ of $\mathcal{T}$. Note that the skewness of $\mathcal{T}$ is equal to $\mathbb{E}\left[(\mathcal{T}-\mathbb{E}[\mathcal{T}])^3\right]/\operatorname{Var}(\mathcal{T})^{\frac{3}{2}}$. In other words, we formulate the optimization problem in the view of the mean, varience, skewness and other high-order quantities of the cumulate time $\sum_{m=1}^{t-1}T_{\rm E2E}(m)$. Additionally, the parameter $\rho>0$ reflects the weight of high-order statistics.

Because the function $\frac{1}{\rho}\ln(*)$ is monotonically increasing, we remove it and focus on an equivalent utility problem as follows:

$$\begin{aligned}\boldsymbol{\mathcal{P}2:}\ &\min_{\{|\mathcal{R}_{\rm r}(t)|,Q(t)\}}\mathbb{E}\left[\exp\left(\rho\sum_{m=1}^{t-1}T_{\rm E2E}(m)\right)\right]\\ &\text{s.t.}\ \ |\mathcal{R}_{\rm r}(t)|\leqslant\left|\Pi^{\rm sel}\right|,\\ &\qquad 1\leqslant Q(t)\leqslant 8,\end{aligned}\tag{10}$$

which can be expanded by Maclaurin series expansion analogously, i.e., $\mathbb{E}[\exp(\rho\mathcal{T})] = 1+\rho\mathbb{E}[\mathcal{T}] + \frac{\rho^2}{2!}\mathbb{E}[\mathcal{T}^2]+\frac{\rho^3}{3!}\mathbb{E}[\mathcal{T}^3]$ for $\mathcal{T}=\sum_{m=1}^{t-1}T_{\rm E2E}(m)$.

It is challenging to solve the minimization problem because of TSN's dynamic network state and the unknown environmental factors of each gateway. Thus, we leverage the principles of multi-armed bandits (MAB) in reinforcement learning to optimize the long-term transmission delay.

5 Risk-sensitive learning strategy for predictive scheduling

For the minimization problem we formulated above, a risk-sensitive learning (RSL) strategy is employed to solve the problem in a static stage and a dynamic stage. The static stage attempts to improve the prediction precision and constrain the number of reserved RBs by selecting sensors through the access history. Then the total delay and the long tail of $T_{\rm E2E}$ are considered in the dynamic stage based on the gradient multi-armed bandits (GMAB) scheme.

5.1 Static stage: sensor selection algorithm

As discussed above, the main task of the static stage is to select the most correlated sensors to compose the reservation sensor candidates set. Obviously, the utilization of reserved RBs is determined by whether the assigned sensors trigger. So a high prediction precision is necessary to reduce the 5G transmission delay. Besides, a salient feature of industrial automation is that the triggering of one event-triggered MTC device may increase the probability that other devices in the vicinity also generate data in quick succession [3,31]. Based on this, calculating the correlation between sensors at two adjacent TTIs is the key to predictively selecting sensors to be reserved. Here we do not care about the relationship between sensors but only concern the correlation between their trigger events. In [3], the naive Bayesian model is applied to learn the correlation of sensors since it simplifies the assumption of conditional independence.

$\boldsymbol{x}(t) = \{x_1(t), x_2(t), \ldots\}$ denotes the set of sensors triggered at TTI $t-1$. We select sensors to make up the reservation candidates set $\boldsymbol{y}(t) = \{y_1(t), y_2(t), \ldots\}(\boldsymbol{x}(t) \cap \boldsymbol{y}(t) = \varnothing)$, which may be triggered at the TTI t with a high probability. Note that the scale of $\boldsymbol{y}(t)$ is not related to the scale of $\boldsymbol{x}(t)$.

In order to explore the correlation between sensors, the access history is used to get the triggering probability of sensor $y_i(t)$ as $\mathbb{P}(y_i(t))(y_i(t) \in \mathcal{S})$, and then three metrics are used to measure the correlation between the set $\boldsymbol{x}(t)$ and the sensor $y_i(t)$ as follows [32].

(1) Conditional probability. Conditional probability at TTI $t-1$ is the probability that sensors out of $\boldsymbol{x}(t)$ will trigger after any sensor in $\boldsymbol{x}(t)$ that has been triggered, which can be obtained by

$$\mathbb{P}_{\mathrm{C}}(y_i(t), \boldsymbol{x}(t)) = \mathbb{P}(y_i(t) \mid x_j(t)) = \sum_{x_j(t) \in \boldsymbol{x}(t)} \frac{\mathbb{P}(y_i(t), x_j(t))}{\mathbb{P}(x_j(t))}, \tag{11}$$

where $\mathbb{P}(y_i(t), x_j(t))$ is the joint probability of $y_i(t)$ and $x_j(t)$ and it is calculated as $\mathbb{P}(y_i(t), x_j(t)) = \mathbb{P}(y_i(t) \mid x_j(t)) \times \mathbb{P}(x_j(t))$.

(2) Mutual information (MI). As described in information theory, MI can measure the development of the triggering probability of $y_i(t)$ after $\boldsymbol{x}(t)$ is triggered, which is given by

$$\mathbb{P}_{\mathrm{MI}}(y_i(t), \boldsymbol{x}(t)) = \sum_{x_j(t) \in \boldsymbol{x}(t)} \mathbb{P}(y_i(t), x_j(t)) \log_2 \frac{\mathbb{P}(y_i(t), x_j(t))}{\mathbb{P}(y_i(t))\mathbb{P}(x_j(t))}, \tag{12}$$

where $\mathbb{P}(y_i(t), x_j(t)) = \mathbb{P}_{\mathrm{C}}(y_i(t), x_j(t)) \times \mathbb{P}(x_j(t))$.

(3) Chi-square (χ^2). Chi-square (χ^2) test is a suitable way to estimate the relevance of two sensors by comparing $\mathbb{P}(y_i(t), x_j(t))$ and $\mathbb{P}(y_i(t)) * \mathbb{P}(x_j(t))$, so as to judge whether these two sensors are dependent. We use χ^2 test metric as below:

$$\mathbb{P}_{\chi^2}(y_i(t), \boldsymbol{x}(t)) = \sum_{x_j(t) \in \boldsymbol{x}(t)} \frac{(\mathbb{P}(y_i(t), x_j(t)) - \mathbb{P}(y_i(t)) \times \mathbb{P}(x_j(t)))^2}{\mathbb{P}(y_i(t)) \times \mathbb{P}(x_j(t))}. \tag{13}$$

The aim of these three metrics is to evaluate the correlation between $y_i(t)$ and $\boldsymbol{x}(t)$. Thus we can select the most relevant sensors to $\boldsymbol{x}(t)$ to be reserved predictively at TTI t for higher resource utilization and lower transmission delay. Thus we use a policy $\Pi^{\mathrm{sel}} = \{\pi_1, \pi_2, \ldots\}$ to select the sensors as follows:

$$\pi_i = \begin{cases} 1, & \text{if } \mathbb{P}(y_i(t), \boldsymbol{x}(t)) \geqslant \alpha, \\ 0, & \text{otherwise.} \end{cases} \tag{14}$$

As we can see from (14), the number of the reserved RBs depends on the threshold α we set, since $\pi_i = 1$ when $\mathbb{P}(y_i(t), \boldsymbol{x}(t)) \geqslant \alpha$. In fact, there exists a trade-off of the number of reserved RBs $|\mathcal{R}_{\mathrm{r}}(t)|$ for the following reasons. If $|\mathcal{R}_{\mathrm{r}}(t)|$ is too small, most of the sensors still need to access the 5G network dynamically with a high handshaking cost, which may violate the time demand of NS data and TC data. On the other hand, if $|\mathcal{R}_{\mathrm{r}}(t)|$ is too big but the prediction precision cannot be guaranteed, the time-frequency resources left will be insufficient for dynamic access sensors. Besides, the reserved resources will also be wasted a lot. Therefore, α is a critical factor to balance this trade-off.

From [3] we know that sensors with lower triggering frequency will obtain a higher ranking in the χ^2 test than in the MI. Based on this, we propose a sensor selection algorithm that is outlined in Algorithm 1 for better practicability. Note that $\boldsymbol{h_i}(t)$ is the i-th element of the history access samples set $\boldsymbol{H}(t)$

Algorithm 1 Sensor selection algorithm (SSA)

Input: Access samples at last TTI $\boldsymbol{x}(t-1) = \{x_1(t-1), x_2(t-1), \ldots\}$, history access samples $\boldsymbol{H}(t) = \{\boldsymbol{h_1}(t), \boldsymbol{h_2}(t), \ldots, \boldsymbol{h}_{|\mathcal{S}|}(t)\}$ with length $|\mathcal{S}|$, $\boldsymbol{y}(t) = \varnothing$;
Output: Predictive select sensors set $\boldsymbol{y}(t) = \{y_1(t), y_2(t), \ldots\}$;
for $i = 1, i \leqslant |\boldsymbol{x}(t)|$ **do**
  if $T(i) \leqslant \beta$ and $y_i(t) \notin \boldsymbol{x}(t)$ **then**
    $\mathbb{P}(y_i(t), \boldsymbol{x}(t)) = \mathbb{P}_{\chi^2}(y_i(t), \boldsymbol{x}(t))$;
  else $\{T(i) > \beta$ and $y_i(t) \notin \boldsymbol{x}(t)\}$
    $\mathbb{P}(y_i(t), \boldsymbol{x}(t)) = \mathbb{P}_{\mathrm{MI}}(y_i(t), \boldsymbol{x}(t))$;
  end if
  if π_i **then**
    $\boldsymbol{y}(t) = \boldsymbol{y}(t) \cup \{y_i(t)\}$;
  end if
end for

with length $|\mathcal{S}|$ at TTI t, and it records the number of the triggering times of the sensor i. And β is the threshold of triggering time used to select a metric.

In a word, we use three different metrics in the static stage to measure the correlation of sensors according to different scenarios, which can improve the precision of sensor selection, and then reduce the delay of the 5G network by multi-priority scheduling based on SPS while considering preemption.

5.2 Dynamic stage: RSL algorithm based on GMAB

As mentioned in Subsection 5.1, the number of reserved RBs $|\mathcal{R}_{\mathrm{r}}(t)|$ brings a trade-off. There are three parameters that are influenced by this trade-off such as the 5G delay, the IPV number of data when it is injected into TSN gateway, and the entire transmission delay under HTSN. Each TSN gateway needs to make decisions based on limited state information at every TTI to find out the optimal policy to dynamically reserve RBs and inject data into its sending queues while guaranteeing the time demands as well. This predictive pre-allocation problem with no prior knowledge is skin to the famous multi-armed bandits' problem [3,33,34], which also concerns the balance of multiple arms' exploration and exploitation to gain the long-term rewards via trying to choose different arms.

We here leverage the GMAB tool to solve the predefined problem since it only focuses on the relative preferences between actions rather than the value of the action itself. In particular, each TSN gateway acts as an agent that selects an action to maximize the long-term rewards. The action set is defined as $\kappa = (k_1, k_2, \ldots, k_{|\kappa|})$, where $k_i = (|\mathcal{R}_{\mathrm{r}}(i)|, Q_i)$ denotes the corresponding action of the i-th arm. The policy gateway made at TTI t is given by $\boldsymbol{\varpi}(t) = \{\varpi_1(t), \varpi_2(t), \ldots, \varpi_{|\kappa|}(t)\}$, which means the agent chooses the i-th arm with probability $\varpi_i(t)$ at TTI t. Here we define the long-term delay in (10) as a utility function $U(t) = -\exp(\rho \sum_{m=1}^{t-1} T_{\mathrm{E2E}}(m))$. The steps of GMAB algorithm are outlined as follows:

(1) Each TSN gateway is given an initial policy: $\boldsymbol{\varpi}(0) = \{\varpi_1(0), \varpi_2(0), \ldots, \varpi_{|\kappa|}(0)\}$ and the preference function $H_{k_i}(t)$ of each action is the same (i.e., $H_{k_i}(0) = 0$ for all i in $|\kappa|$).

(2) At every TTI t, each TSN gateway selects actions according to the policy updated at TTI $t-1$, and then obtains a utility function $U(t) = -\exp(\rho \sum_{m=1}^{t-1} T_{E2E}(m))$ as the reward of the actions selected.

(3) Then, TSN gateway calculates each action's probability by a soft-max distribution based on the preference function got before:

$$\Pr\{k_i = (|\mathcal{R}_{\mathrm{r}}(i)|, Q_i)\} \doteq \frac{\mathrm{e}^{H_{k_i}(t-1)}}{\sum_{j=1}^{|k|} \mathrm{e}^{H_{k_j}(t-1)}} \doteq \varpi_{k_i}(t-1) \tag{15}$$

and gets the new policy $\boldsymbol{\varpi}(t)$.

(4) Subsequently, each TSN gateway updates the preference of actions by

$$\begin{aligned} &H_{k_i}(t) \doteq H_{k_i}(t-1) + \eta(U(t-1) - \bar{U}(t-1))(1 - \varpi_{k_i}(t-1)), && \text{and} \\ &H_{k_j}(t) \doteq H_{k_j}(t-1) - \eta(U(t-1) - \bar{U}(t-1))\varpi_{k_j}(t-1), && \text{for all } k_j \neq k_i, \end{aligned} \tag{16}$$

where $\eta > 0$ is a step-size parameter and $\bar{U}(t)$ is the average rewards up to TTI $t-1$, which can be computed incrementally [35].

(5) TSN gateway iteratively updates its policy $\boldsymbol{\varpi}(t)$ severally and makes new decisions abide by the latest policy so that the likelihood of choosing the optimal action is proportional to its rewards.

Since we take high-order quantity into account when we formulate the minimization problem, the tail of transmission delay is optimized as well as the optimal policy is learned via reinforcement learning.

Table 2 Proportions of sensors' trigger events

Proportion	NS data (%)	TC data (%)	BE data (%)
Proportion 1	6	40	54
Proportion 2	4	40	56
Proportion 3	2	40	58
Proportion 4	2	50	48
Proportion 5	2	30	68

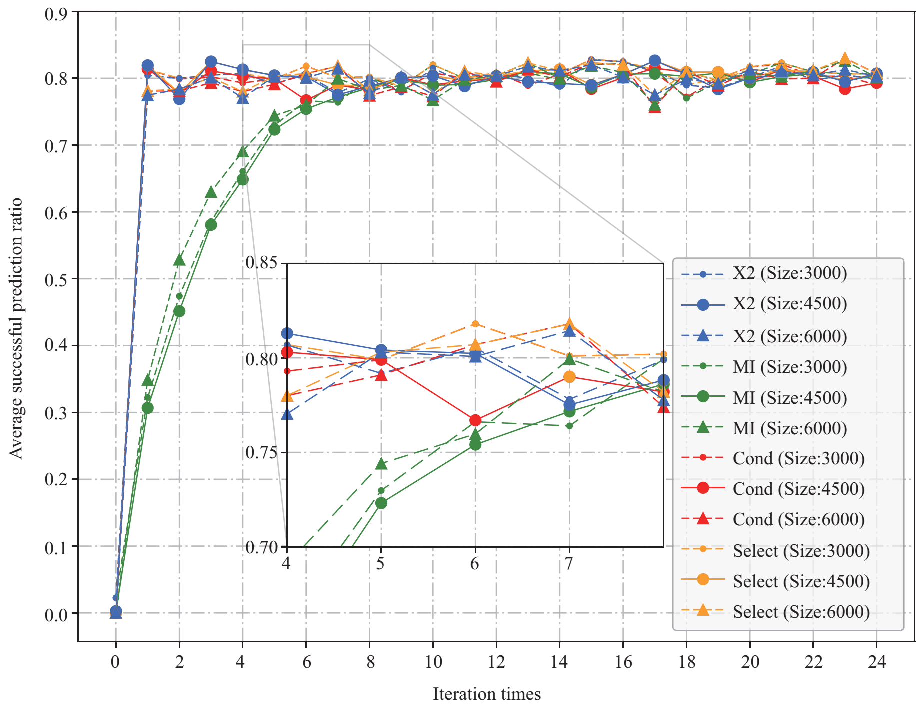

Figure 6 (Color online) The prediction performance of different correlation metrics.

6 Numerical results

6.1 Sensor prediction simulation

In this subsection, we evaluate the performance of the proposed HTSN architecture based on data with a stringent deadline, which is generated by monitoring sensors deployed along the hot rolling line. Sensors for monitoring temperature, humidity, pressure and so on are randomly distributed to sense the manufacturing process to provide robust control via closed-loop feedback. Sensors activate periodically and generate TC data, which are the main data we care about. Event-triggered sensors such as camera and vibration sensors only activate as long as there occur safety emergencies. They generate burst NS data, which have the highest priority and can preempt TC data.

Here, data from different processes with their particular transmission deadline are transmitted in turns. What we need to do is to learn the correlation between sensors and ignore the interference brought by sensors that with no relationships. We consider the proportion of sensors' trigger events as in Table 2.

The performance of the predictive SSA is evaluated in terms of prediction accuracy (successful prediction ratio). We compare the performance of three correlation metrics (X2: chi-square test, MI: mutual information, Cond: conditional probability) and the sensor selection algorithm we proposed on three sizes (3000, 4500, 6000) of data. Figure 6 shows how different correlation metrics diverse in the performance of prediction accuracy. It is obvious that the X2 metric, as well as the Cond metric, has the best performance when the iteration times are few. The prediction accuracy of MI is much lower than the other two. But after several iterations, the difference between these three metrics' performance is inconspicuous, and the prediction accuracy of them all converges to 0.8. Since the SSA algorithm we proposed chooses the metric by thresholds α and β, its performance is as good as the best metric. The

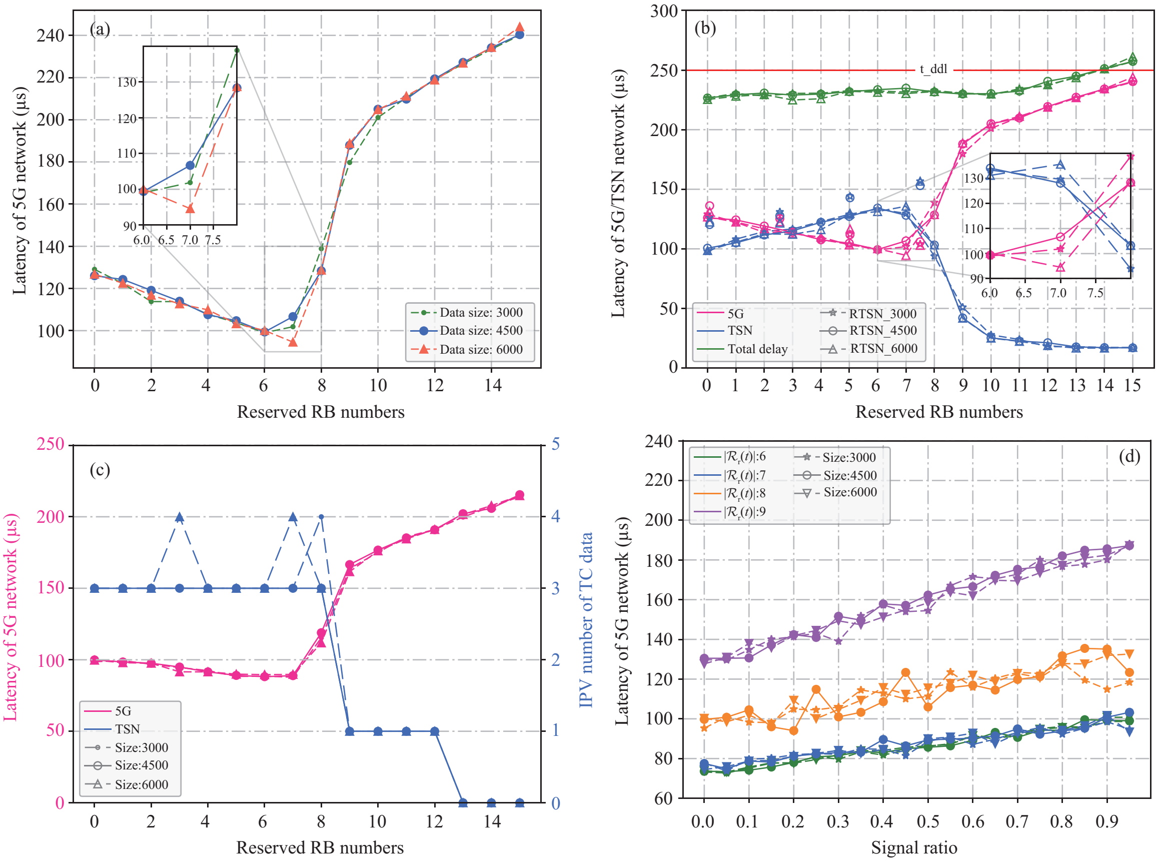

Figure 7 (Color online) The varies of 5G delay (a), 5G and TSN delay (b), data IPV and 5G delay (c) with $|\mathcal{R}_{\rm r}(t)|$. (d) The varies of 5G delay with signal ratio.

high prediction accuracy guarantees the resource utilization of 5G and lays the foundation for the HTSN architecture.

6.2 HTSN simulation

Since the 5G network and TSN are coupled and interacted, the main influence factor of HTSN is the number of reserved RBs $|\mathcal{R}_{\rm r}(t)|$. Thus, we simulate the relationship between $|\mathcal{R}_{\rm r}(t)|$ and delay of 5G/TSN. Figure 7(a) shows that as $|\mathcal{R}_{\rm r}(t)|$ growing, the delay of the 5G network decreases first and then increases. The lowest point of the delay curve is the trade-off point we mentioned in Subsection 5.1, which is because the prediction accuracy cannot reach 100%, and thus, assigning sensors in advance would cause the waste of radio resources. Here we set the total number of subslot to 15, and the performance of the pre-allocation mechanism is optimal when $|\mathcal{R}_{\rm r}(t)| = 7$ as we can see from Figure 7(b). What is more, the reason why the delay of the 5G network increases rapidly after the trade-off point is the limitation of the radio resources. The more $|\mathcal{R}_{\rm r}(t)|$ is reserved, the more resource is wasted accordingly, and the fewer resources used for dynamic access, the lower reliability of transmission.

Based on the dynamic injection mechanism of the TSN queue, the indeterminacy of transmission caused by the 5G network can be made up by the TSN to meet the strict transmission requirements of intelligent manufacturing. Figure 7(b) shows the interaction of 5G and TSN as $|\mathcal{R}_{\rm r}(t)|$ growing. It can be seen that the delay of 5G and TSN has a near-ideal negative correlation via adjusting the IPV of TC data adaptively. Given the deadline $= 250$ µs, the TSN tries to save as many resources as it can under the premise of not violating the deadline of the total delay under HTSN. Obviously, the data injection mechanism we proposed makes up for the shortcoming of the 5G network perfectly and improves the determinacy since it scarcely violates the deadline.

To further analyze the relationship between TSN queue and 5G delay, we give Figure 7(c), from which we can see that the IPV number of data and the 5G network delay also have a similar negative correlation. Since the IPV number of data is always identical to gate ID and directly proportional to its TSN delay,

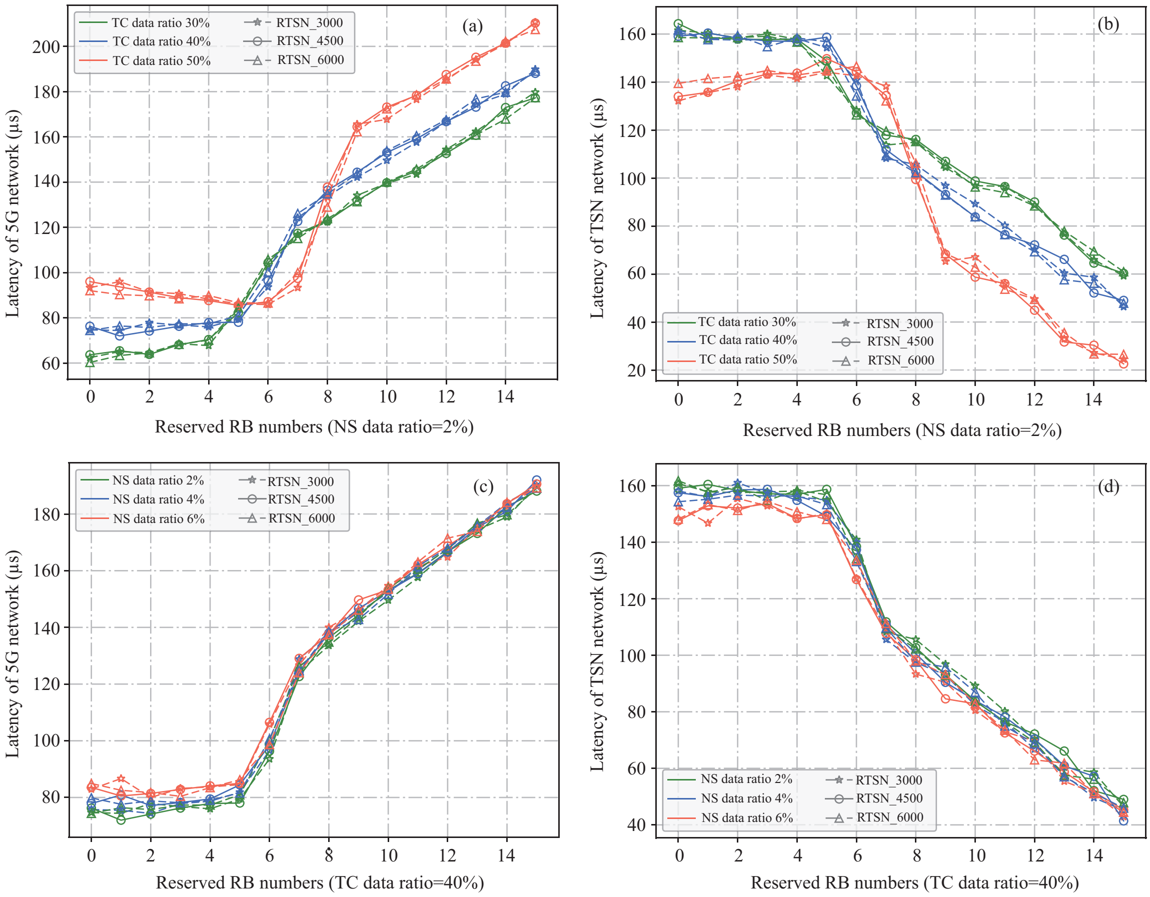

Figure 8 (Color online) The comparison of different types of filed data with different proportions. 5G delay (a) and TSN delay (b) with different TC data ratios; 5G delay (c) and TSN delay (d) with different NS data ratios.

the general trends of the queue priority curve and TSN delay curve are analogous. However, there are some step-changes of the IPV number as it is an integer. It can be concluded that although we arrange an IPV number between 0 and 8, we cannot assign 5G data to the queue corresponding to IPV 8 since the scheduling capability of the 5G network is not enough to realize low-latency high-reliability transmission by itself.

Except for $|\mathcal{R}_{\mathrm{r}}(t)|$, the ratio of signaling transmission is also a critical factor that influences the SPS within the 5G network and the total delay of HTSN. Here, we formulate the extra delay caused by signaling as a signal ratio and plot the relationship between it and the 5G delay. As shown in Figure 7(d), we select $|\mathcal{R}_{\mathrm{r}}(t)|$ from 6 to 9 according to Figure 7(a). It can be seen that no matter $|\mathcal{R}_{\mathrm{r}}(t)|$ is larger than, equal to, or less than the trade-off point, the delay of 5G network increases with the increase of signal ratio. This is because $|\mathcal{R}_{\mathrm{r}}(t)|$ has nothing to do with the number of TC data; there always exist TC data to be dynamically scheduled due to the inaccuracy of prediction, so the increase of signal ratio will lead to the increase of the 5G network's delay.

Lastly, the types of field data can influence the latency of the co-design 5G and TSN network as well. According to Table 2, we give the comparison of different types of data with different proportions in Figure 8. It can be seen that the 5G delay increases as the TC data ratio grows in Figure 8(a), and the TSN delay decreases in Figure 8(b) accordingly. Moreover, the trade-off point moves to the right with a higher proportion of TC data. This is because that we need more reserved resources to achieve low-latency communication if the predictive accuracy does not change. The variation trends of 5G delay and TSN delay are analogous in Figures 8(c) and (d), which is due to the increase of data as the NS data ratio grows.

6.3 Risk-sensitive learning simulation

To deal with the tail of the 5G delay, we use a risk-sensitive utility function to optimize expectations and high-order quantities of accumulative integrated delay of HTSN. The proposed HTSN architecture

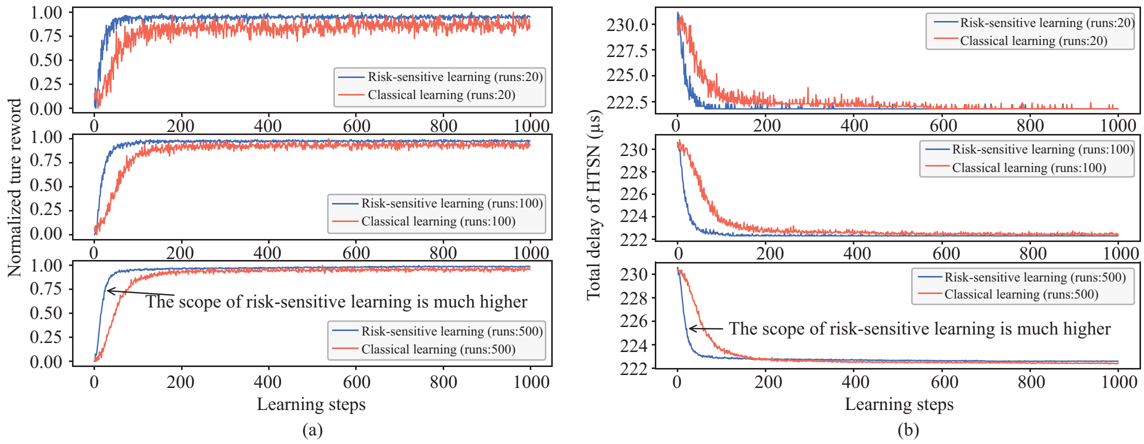

Figure 9 (Color online) (a) The normalized reward of risk-sensitive reinforcement learning with different run times; (b) the total delay of HTSN with different learning run times.

is evaluated as an integral in Figure 9(a), which delineates the improvement brought by the risk-sensitive utility. We repeat GMAB learning for three sizes (20, 100, 500) of independent runs, and for each run we measure its performance with experience over 1000 time steps. With the increase of repetitions, the risk-sensitive learning curve is more stable, and the learning reward is getting closer to the normalized true reward. It means that the learning rate of risk-sensitive learning is faster than classical learning. Besides, with the increase of iteration times, the convergence rate of risk-sensitive learning is faster.

As for the performance of the total delay shown in Figure 9(b), the curve of risk-sensitive learning is steeper than the classical one, which means that the high-order quantities are optimized while learning, and the delay distribution of HTSN is more centralized with a shorter tail. It proves the risk-sensitive reinforcement learning strategy we proposed works and improves the transmission reliability.

7 Conclusion

In this paper, we proposed HTSN, a heterogeneous architecture that co-designs 5G and TSN to provide deterministic transmission from the industrial field to the remote data center with wireless access and wired forwarding. Within the 5G network, a preemption-considered multi-priority wireless scheduling mechanism was proposed to satisfy the diverse QoS requirements of field data by exploring the triggering correlation between uplink sensors in industrial process automation. To offset the time deviation caused by the 5G network, an adaptive data injection mechanism of the TSN gateway queue was developed here to reduce the total delay under HTSN. Then we formulated a risk-sensitive utility function, which takes the high-order quantities of the total delay into account. Finally, a risk-sensitive reinforcement learning based on GMAB was executed and thus the determinacy of HTSN is improved.

Acknowledgements This work was partially supported by National Key Research and Development Program of China (Grant No. 2018YFB1702100) and National Natural Science Foundation of China (Grant Nos. 62025305, 61933009, 62103272).

References

1 Zhou J L, Li L Y, Vajdi A, et al. Temperature-constrained reliability optimization of industrial cyber-physical systems using machine learning and feedback control. IEEE Trans Automat Sci Eng, 2021. doi: 10.1109/TASE.2021.3062408
2 Zhou X K, Liang W, Shimizu S, et al. Siamese neural network based few-shot learning for anomaly detection in industrial cyber-physical systems. IEEE Trans Ind Inf, 2021, 17: 5790–5798
3 Li M Y, Guan X P, Hua C Q, et al. Predictive pre-allocation for low-latency uplink access in industrial wireless networks. In: Proceedings of IEEE International Conference on Computer Communications, Honolulu, 2018. 306–314
4 Li M Y, Chen C L, Hua C Q, et al. A learning-based pre-allocation scheme for low-latency access in industrial wireless networks. IEEE Trans Wireless Commun, 2020, 19: 650–664
5 Farkas J, Varga B, Mikloòs G, et al. 5G-TSN integration meets networking requirements for industrial automation. Ericsson Technology Review, 2019. https://www.ericsson.com/en/reports-and-papers/ericsson-technology-review/articles/5g-tsn-integration-for-industrial-automation
6 Fu S, Wu J S, Wen H, et al. Software defined wireline-wireless cross-networks: framework, challenges, and prospects. IEEE Commun Mag, 2018, 56: 145–151
7 Ke C H, Chen Y S, Yu Y S. Improving video transmission in software defined wired and wireless networks using multi-path transmission. J Commun Netw, 2017, 19: 587–595
8 Cai L, Shen X S, Mark J W, et al. QoS support in wireless/wired networks using the TCP-friendly AIMD protocol. IEEE Trans Wireless Commun, 2006, 5: 469–480

9 Underberg L, Kays R, Dietrich S, et al. Towards hybrid wired-wireless networks in industrial applications. In: Proceedings of IEEE Industrial Cyber-Physical Systems (ICPS), Saint Petersburg, 2018. 768–773

10 Sachs J, Wallstedt K, Alriksson F, et al. Boosting smart manufacturing with 5G wireless connectivity. Ericsson Technology Review, 2019. https://www.ericsson.com/en/reports-and-papers/ericsson-technology-review/articles/boosting-smart-manufacturing-with-5g-wireless-connectivity

11 Lyons T J. Stochastic finance: an introduction in discrete time. Math Intelligencer, 2004, 26: 67–68

12 Batewela S, Liu C F, Bennis M, et al. Risk-sensitive task fetching and offloading for vehicular edge computing. IEEE Commun Lett, 2020, 24: 617–621

13 Bennis M, Debbah M, Poor H V. Ultrareliable and low-latency wireless communication: tail, risk, and scale. Proc IEEE, 2018, 106: 1834–1853

14 Yang G, Xiao M, Poor H V. Low-latency millimeter-wave communications: traffic dispersion or network densification? IEEE Trans Commun, 2018, 66: 3526–3539

15 Vu T K, Liu C F, Bennis M, et al. Path selection and rate allocation in self-backhauled mmWave networks. In: Proceedings of IEEE Wireless Communications and Networking Conference, Barcelona, 2018. 1–6

16 Vu T K, Liu C F, Bennis M, et al. Ultra-reliable and low latency communication in mmWave-enabled massive MIMO networks. IEEE Commun Lett, 2017, 21: 2041–2044

17 Assaad M, Ahmad A, Tembine H. Risk sensitive resource control approach for delay limited data in wireless networks. In: Proceedings of IEEE Global Telecommunications Conference, Houston, 2011. 1–5

18 Alsenwi M, Tran N H, Bennis M, et al. eMBB-URLLC resource slicing: a risk-sensitive approach. IEEE Commun Lett, 2019, 23: 740–743

19 Holfeld B, Wieruch D, Wirth T, et al. Wireless communication for factory automation: an opportunity for LTE and 5G systems. IEEE Commun Mag, 2016, 54: 36–43

20 3GPP, ETSI. Evolved Universal Terrestrial Radio Access (E-UTRA) and Evolved Universal Terrestrial Radio Access Network (E-UTRAN). ETSI TS 136 300 V11.6.0 (2013-07). https://www.etsi.org/deliver/etsi_ts/136300_136399/136300/11.06.00_60/ts_136300v110600p.pdf

21 Schulz P, Matthe M, Klessig H, et al. Latency critical IoT applications in 5G: perspective on the design of radio interface and network architecture. IEEE Commun Mag, 2017, 55: 70–78

22 Seo J B, Leung V C M. Performance modeling and stability of semi-persistent scheduling with initial random access in LTE. IEEE Trans Wireless Commun, 2012, 11: 4446–4456

23 Afrin N, Brown J, Khan J Y. Design of a buffer and channel adaptive LTE semi-persistent scheduler for M2M communications. In: Proceedings of IEEE International Conference on Communications, London, 2015. 5821–5826

24 Soleymani D M, Puschmann A, Roth-Mandutz E, et al. A hierarchical radio resource management scheme for next generation cellular networks. In: Proceedings of IEEE Wireless Communications and Networking Conference Workshops, Doha, 2016. 416–420

25 Raza M, Le-minh H, Aslam N, et al. A novel MAC proposal for critical and emergency communications in industrial wireless sensor networks. Comput Electr Eng, 2018, 72: 976–989

26 Farag H, Sisinni E, Gidlund M, et al. Priority-aware wireless fieldbus protocol for mixed-criticality industrial wireless sensor networks. IEEE Sens J, 2019, 19: 2767–2780

27 Gaj P, Jasperneite J, Felser M. Computer communication within industrial distributed environment—a survey. IEEE Trans Ind Inf, 2013, 9: 182–189

28 Zand P, Chatterjea S, Das K, et al. Wireless industrial monitoring and control networks: the journey so far and the road ahead. J Sens Actuator Netw, 2012, 1: 123–152

29 Lin F L, Dai W B, Li W B, et al. A framework of priority-aware packet transmission scheduling in cluster-based industrial wireless sensor networks. IEEE Trans Ind Inf, 2020, 16: 5596–5606

30 Hang N T T, Trinh N C, Ban N T, et al. Delay and reliability analysis of p-persistent carrier sense multiple access for multi-event industrial wireless sensor networks. IEEE Sens J, 2020, 20: 12402–12414

31 Shafiq M Z, Ji L, Liu A X, et al. Large-scale measurement and characterization of cellular machine-to-machine traffic. IEEE/ACM Trans Networking, 2013, 21: 1960–1973

32 Singh S R, Murthy H A, Gonsalves T A. Feature selection for text classification based on gini coefficient of inequality. In: Proceedings of the Fourth Workshop on Feature Selection in Data Mining, Hyderabad, 2010. 76–85

33 Arora P, Szepesvári C, Zheng R. Sequential learning for optimal monitoring of multi-channel wireless networks. In: Proceedings of IEEE International Conference on Computer Communications, Shanghai, 2011

34 Xu Q, Zheng R. When data acquisition meets data analytics: a distributed active learning framework for optimal budgeted mobile crowdsensing. In: Proceedings of IEEE INFOCOM-IEEE Conference on Computer Communications, Atlanta, 2017. 1–9

35 Sutton R S, Barto A G. Reinforcement Learning: An Introduction. Cambridge: MIT Press, 2018